Analysis of resonant responses of split ring resonators using conformal mapping techniques.

Scott G McMeekin,

Department of Electrical and Electronic Engineering, School of Science Engineering and Design, Glasgow Caledonian University, Cowcaddens Road, Glasgow, G4 0BA, United Kingdom

Ali Z. Khokhar, Basudev Lahiri, Richard M. De La Rue and Nigel P. Johnson.

Department of Electrical and Electronic Engineering, University of Glasgow, Oakfield Avenue, Glasgow, G12 8QQ, United Kingdom

ABSTRACT.

We report a novel method for modeling the resonant frequency response of infra-red light, in the range of 2 to 10 microns, reflected from metallic spilt ring resonators (SRRs) fabricated on a silicon substrate. The calculated positions of the TM and TE peaks are determined from the plasma frequency associated with the filling fraction of the metal array and the equivalent LC circuit defined by the SRR elements. The capacitance of the equivalent circuit is calculated using conformal mapping techniques to determine the co-planar capacitance associated with both the individual and the neighbouring elements. The inductance of the equivalent circuit is based on the self-inductance of the individual elements and the mutual inductance of the neighboring elements.

The results obtained from the method are in good agreement with experimental results and simulation results obtained from a commercial FDTD simulation software package. The method allows the frequency response of a SRR to be readily calculated without complex computational methods and enables new designs to be optimised for a particular frequency response by tuning the LC circuit.

KEYWORDS: Metamaterials, optics, optical simulation, integrated optics.

1. INTRODUCTION.

Much attention has focused on a specific class of metamaterials[1] with the potential of possessing a negative permittivity, ε and negative permeability, μ enabling them to achieve negative refraction[2] and to be exploited for a wide range of novel applications including perfect lensing[3]. Optical metamaterials are typically formed from an array of elements whose dimensions are in the order of one tenth of the wavelength of the light with which they interact. A common element used to form the metamaterial array is the Split Ring Resonator (SRR), which shows a strong dependence on the orientation of the polarization of the incident light with respect to the orientation of the geometry of the SRRs. To achieve a true negative index in the material, both the permittivity, ε, and the permeability, μ, of the material should go negative over the same frequency range. When this condition is satisfied the material can be classified as a "left handed" and is often referred to as a Negative Index Material or NIM. The condition can be satisfied with in-plane incident geometries[4,5] with simple planar arrays of split ring resonators, however, light incident to the normal of the surface shows a distinct difference in the spectrum of reflected and transmitted light as the polarization of the light is altered[6].

Figure 1 shows a typical array of SRR elements comprising of gold rings on a silicon substrate. The array of SRR elements will interact with the incident light through two separate mechanisms to produce resonant peaks and troughs in

the spectrum of the reflected and transmitted light respectively. The first resonant peak in the spectrum of reflected light that is of interest is related to the dilute plasma frequency of the metal film from the SRR elements and is largely independent of the polarization of the incident light. The peak is referred to as the Mie resonance[7]. The second resonant peak, which is at a lower frequency relative to the plasmon resonant peak, is strongly dependent upon the polarization of the incident light. This peak is commonly attributed to the resonance of the LC equivalent circuit that each of the individual element of the array forms. Recent work has attributed the second resonant peak to higher order plasmon resonances[8], however, a more complete analysis of the effective inductance and capacitance of the SRR elements, presented here, supports the assumption that the peak is associated with an electrical LC resonance and not a higher order plasmon resonance.

The LC equivalent circuit is formed by the capacitance from the gap in the ring while the almost single-turn metal ring forms the inductor[5]. With the electric field polarized parallel to the SRR gap a potential difference will be created between the opposite face of the SRR gap resulting in a current flow round the ring and an induced inductance around the ring and capacitance across the gap. If the polarization of the incident light is rotated such that the electric field is perpendicular with the gap, no potential difference will be induced across the gap and no charge will flow around the ring and hence the resonant peak associated with the LC resonance will disappear. A similar effect can be obtained by closing the gap in the SRR rings resulting in no LC resonant peak in the reflection spectrum of the incident light.

By controlling the inductance or capacitance of the SRR elements it would be possible to tune the resonant frequency of the LC peak. Steps towards controlling the resonant response will be important to add functionality to the SRR array and will enable new applications to be developed. Developing a fuller understanding of the dependence of the capacitance and inductance of the SRR element upon the design and layout of the SRR layout will enable a better physical understanding.

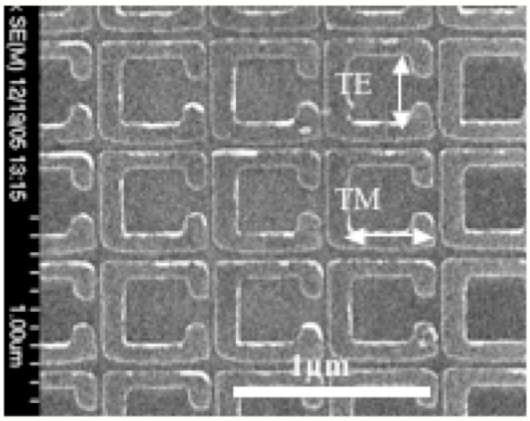

Figure 1. Micrograph of a typical SRR array with gold elements on a Silicon substrate showing the orientation of the TE and TM polarisations for a LC resonant response.

Computational techniques used to model the resonant response of a SRR array include FDTD[9] and finite element models[10] which simulates the electromagnetic field distribution as a function of time and space as a result of the specified dispersive permittivity response of the metal film. These computational simulation techniques have been demonstrated to provide an accurate simulation of the reflection and transmission spectrum from a range of SRR designs and provide an analysis of the electrical field distribution around the structure and can be a useful tool in determining how the electromagnetic field interacts with the SRR elements. However these complex simulation techniques tend to be computationally intense and do not provide an understanding of the complex relationship between capacitance and inductance of the elements and the physical design and layout of the SRR array.

The development and use of equivalent LC circuit models has received little attention in the literature in comparison with the computational simulation techniques, despite the common reference in the literature of the longer wavelength

peak being related to the LC resonance of the SRR element. The standard reference for the inductance of the SRR ring is the simplified calculation of a wire wound coil while the capacitance of the element is modeled as a parallel plate capacitance formed from the opposite faces of the gap in the SRR element. However this simplistic approach does not take into account all the capacitive and inductive components formed by the SRR elements and does not provide an accurate LC equivalent circuit to determine resonant response of the array. A more complete analysis of the LC equivalent circuit is given below which takes into account the effect of adjacent SRR elements.

2. LC RESONANCE ANALYSIS FOR A SRR RING.

To provide an accurate model of the LC resonance for the SRR array it is necessary to identify all the inductive and capacitive components that will contribute to the equivalent circuit model. By analysing the charge distribution and the charge flow around the SRR element, shown schematically in Figure 2, we can identify the following inductive components 1) a charge flow around the rectangular loop will form a self inductance element, L_{Ring}, and 2) the charge flowing in opposite directions in the arms of two adjacent elements will form a mutual inductance, L_{mut}. Similarly we can identify the following capacitive components 1) the differential potential difference formed by the charge distribution across the gap of the SRR element will form a capacitance that can be separated into a parallel plate component formed by the opposite faces and a coplanar component formed by the finite width conductors on the silicon substrate, $C_{G\text{-}PP}$, and $C_{G\text{-}CP}$ respectively, and 2) the opposite charge on the arms of two adjacent elements will form capacitance between the with a parallel plate and coplanar capacitive component, $C_{EE\text{-}PP}$ and $C_{EE\text{-}CP}$ respectively.

The high frequency current flow and charge distribution around the SRR elements shown in Figure 2 will be induced only when the TE field is parallel to the gap in the SRR element. If the polarisation is rotated so the TE field is perpendicular to the gap there will no potential difference induced across the gap and no charge will flow around the ring.

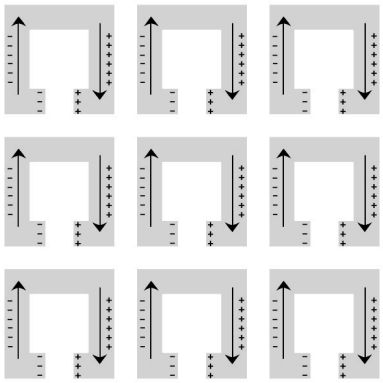

Figure 2. Schematic showing the charge flow and distribution between the SRR gap and adjacent SRR elements.

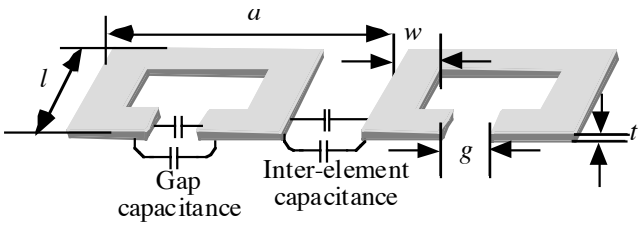

Figure 3. Schematic showing the co-planar and parallel plate capacitances for SRR array that is infinite in both in-plane dimensions.

The excitation frequency at which the incident light is equal to the resonance of the LC circuit is given by the standard equation for an LC resonant circuit given by:

$$\omega_{LC} = \frac{1}{\sqrt{L_T C_T}}. \tag{1}$$

where L_T and C_T are the total inductance and capacitance formed for a single SRR element and the adjacent elements.

The total inductance of the SRR is formed by the by the self-inductance of the ring in series with the mutual inductance formed by the parallel rectangular conductors of the adjacent rings. An approximation for the self-inductance of a complete rectangular loop made from rectangular cross-section wire is given by[11]:

$$L_{Ring} = 0.2\mu_o \left(-\frac{w}{2}\sinh^{-1} 1 + \frac{w}{2}\sqrt{2} + \left(l - \frac{w}{2}\right)\sinh^{-1}\left(\frac{l - \frac{w}{2}}{w/2}\right) - \sqrt{\left(l - \frac{w}{2}\right)^2 + \left(\frac{w}{2}\right)^2} \right) \quad H. \tag{2}$$

An approximation for the mutual inductance of two parallel rectangular conductors is given by[12]:

$$L_{Mutual} = 0.2.l\left(\ln\left(\frac{l}{d} + \sqrt{1 + \frac{l^2}{d^2}}\right) - \sqrt{1 + \frac{d^2}{l^2}} + \frac{d}{l} \right) \quad \mu H. \tag{3}$$

where, referring to Fig. 2, l is the length of the SRR element, w is the width of the wire forming the split ring, t is the thickness of the wire - and d is the centre-to-centre separation between the arms of adjacent SRR elements.

Previously only the parallel plate capacitance of the gap in the SRR element has been taken into account when considering the capacitance of the SRR array[5]. However, due to the proximity of the individual SRR elements to each other, it is necessary to consider the capacitance between the individual elements. It is necessary to take into account not only the parallel plate but also the coplanar capacitances formed between both the individual SRR elements, C_{EE}, and the capacitance formed by the gap in the SRR structure, C_G. The parallel plate capacitance of both components can be calculated from the standard equation:

$$C_{G-PP} = \varepsilon_o \varepsilon_r \frac{w.t}{g} \quad and \quad C_{EE-PP} = \varepsilon_o \varepsilon_r \frac{l.t}{a - l} \quad F \tag{4a) and (4b)}$$

The coplanar capacitance can be calculated by using conformal mapping techniques to take into account the field that is present in the substrate. The general form of the equation for the coplanar capacitance per unit length for two metal strips of width p, separated by distance q, is given by[13]:

$$C_{cp} = \frac{(\varepsilon_r + 1)\varepsilon_o}{2} \frac{1}{\pi} \ln\left[2\frac{1 + \sqrt{k'}}{1 - \sqrt{k'}} \right] \quad F/m \tag{5}$$

where k' is a geometrical factor given by:

$$k' = \sqrt{\left(1 - \left(\frac{p}{p + 2q}\right)^2\right)}. \tag{6}$$

For the coplanar capacitance across the gap *p* is given by the gap length, *g*, and *q* is given by the length of the short arms, *(l-g)/2*. For the coplanar capacitance between the SRR elements p is given by the separation between the elements, *(a-l),* and *q* is given by the width, *w*.

For an SRR array with a period significantly larger than the size of the SRR element the total inductance capacitance of the array will be determined by the self inductance of the square coil and the capacitance formed across the gap in the SRR. As the spacing between the SRR elements decrease the mutual inductance and capacitance will increase and dominate over the self-inductance of the SRR element.

3. PLASMA FREQUENCY

The shorter wavelength peak in the reflectance spectrum shown in Figure. 1 can be identified as the reduced plasma frequency[14] and is a collective property of the dilute metal film forming the SRR array. This resonance has relatively low dependence on shape and, at frequencies in the infra-red part of the spectrum, is also not strongly dependent on the particular metal used. An expression for the resonant plasma frequency of an array of metal columns has been developed from the bulk value of the plasma frequency of a metal which takes account of the reduced electron density and enhanced effective electron mass[10]. The resonant frequency of the peak is dependent upon the dilution of the metal and is inversely proportional to the natural logarithm of the filling fraction given by the ratio of the period of the array to the radius of extended cylindrical pillars and is given by[15]:

$$\omega_p^2 = \frac{c^2.2\pi}{a^2.\ln(a/r)} \qquad \text{rad s}^{-1}. \tag{7}$$

To take into account the more complex geometry of the SRR elements - and the fact that they are closely packed - a geometric factor F is introduced, which is the area of exposed silicon in a unit cell, i.e the total area of the unit cell minus the area covered by the metallic SRR and given by:

$$F = a^2 - \left[l^2 - (l - 2.w)^2 - (g.w)\right] \tag{8}$$

A modified expression for the reduced plasma frequency may then be written as:

$$\omega_p^2 = \frac{c^2.2\pi}{a^2.\ln\left(a^2/F\right).n_{eff}^2} \qquad \text{rad s}^{-1}. \tag{9}$$

where n_{eff} is the effective refractive index of the dielectric medium at the frequency of the infra-red radiation interacting with the SRR array. The value of n_{eff} is approximately 70% of the value of silicon and is related to the distribution between silicon and air of the electric flux density interacting with the SRR array. As the metal area of an individual SRR increases, for a fixed unit cell area, *F* decreases - and the plasma frequency also decreases. This effect is greatest at the smallest spacing between SRRs, where the position of the peak diverges substantially from the simple theory.

4. EXPERIMENTAL VERIFICATION

SRRs were fabricated using gold, aluminium and silver on a silicon substrate and the refection spectrum measured to identify the Mie and LC resonant peaks. Silicon was selected for the substrate due to the potential of integrating with electronic or optoelectronic elements on the substrate to form an active metamaterial. The SRRs were designed to have an LC resonance in the range of 2 to 10 microns

The reflection spectrum from the aluminium SRR, shown in Figure 4a), is typical of the samples fabricated. For TE polarisation, with the electric field oriented across the SRR gaps, two reflectance peaks are observed for the particular

structure being measured: the sharper Mie resonance occurs at around a 3 µm wavelength, while the broader LC peak is observable at around 8 µm. The spectrum shown in Figure 4 b), simulated using Rsoft Fullwave FDTD software[16], provides good correlation with the experimental data with comparable values for the resonant wavelengths and a similar shape to the peaks. Other features to note are the line-width of the Mie resonance (the shorter wavelength peaks) in the two orthogonal polarisations. The peak is wider by around a factor of two for TM excitation in comparison with TE polarisation.

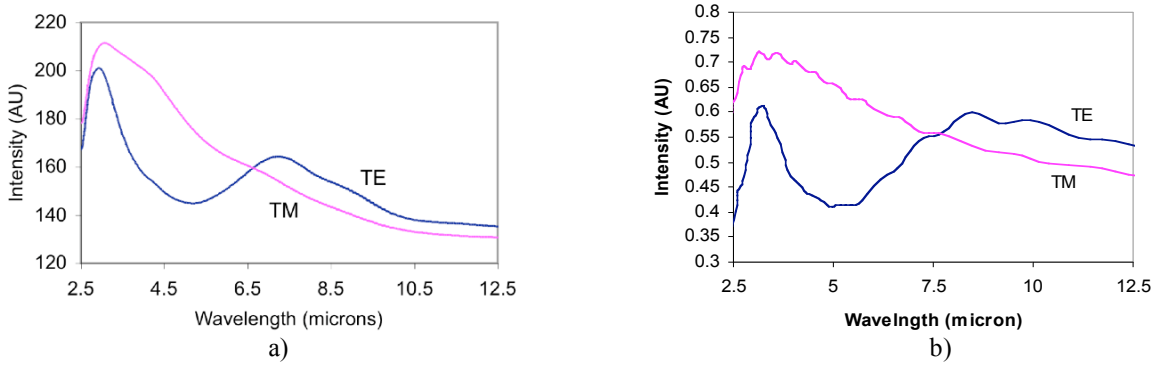

Figure 4. Reflectance spectra for aluminium sample showing: a) experimental and b) simulated TE and TM resonant peaks.

In Table 1 the experimental values of the shorter wavelength Mie resonant peak and the longer wavelength LC resonant peak for all the samples are compared with the values calculated using FDTD simulations and the values calculated using the equivalent circuit analysis presented above. Agreement is typically within 10 %, but diverges for smaller separation between elements to 20%. In general, the peak resonant wavelengths for the experimental results are at shorter wavelengths than either simulations or the models. Over the experiment results, simulations and equivalent circuit analysis there is little effect produced by changing the metal at these wavelengths.

	Dimensions of SRRs (nm)					**TE Polarisation Resonant Wavelengths (micron)**					
metal	l	w	g	a	t	Mie 1 (µm)			LC (µm)		
						Exp	FDTD	Plasma Resonance	Exp	FDTD	LC Resonance
Au	552	90	22	614	30	3.5	4.2	3.2	10	12.5	9.9
Au	217	66	33	297	30	1.3	1.6	1.5	3.1	4.3	2.7
Ag	572	118	120	667	30	3.0	3.2	3.5	8.2	8.5	8.8
Al	564	120	130	616	30	3.0	3.1	3.6	8.2	8.6	8.6
Al	564	120	130	664	30	2.9	3.1	3.5	8.1	8.5	8.5

Table 1. Comparison of peak resonant wavelengths for SRR of various metals from experimental measurement, FDTD simulation and calculated from the Mie and LC resonance. The metal thickness for all samples is nominally 30 nm.

Comparing the experimental, FDTD and calculated results indicates that the equations presented for the reduced plasma frequency and the LC frequency are valid across the range of geometries investigated and provide a simple method of analysing the optical response of the SRR array based on the design and the related equivalent electrical circuit.

The equations have been used to investigate the dependence of the resonant Mie and LC peaks on the shape of the SRR element. The width, l_x, and the length, l_y, of the SRR were varied with fixed aspect ratio and independently and the resonant wavelengths were calculated using the dilute plasma equation (9) and the equivalent electric circuit. In Figure 5 a) both l_x and l_y are varied by an equal amount such that the SRR remains square, in Figure 5 b) l_x is varied while l_y is constant at 564 nm and in Figure 5 c) l_y is varied while l_x is constant at 564 nm. Comparing Figure 5 b) with 5 c) we can identify a stronger dependence of the LC resonant peak on the width of the SRR than on the length of the SRR. This can

be attributed to the fact the coplanar capacitance across the SRR gap is dependant on the width of the SRR and not the length. The parallel plate capacitance across the SRR gap is independent of both length and width of the SRR and will remain for both scenarios. The increase in LC resonant wavelength in Figure 5 c) is due to an increase in the mutual and self-inductance of the SRR and the mutual capacitance between the neighbouring SRR elements. Figures 5 b) and c) show that the Mie resonant peak is independent of the orientation of the dimensional changes as the dilute plasma frequency is dependent on the area of metal rather than the specific SRR shape. Figure 5 a) shows the strongest dependence of both the Mie and LC resonant peaks occurs when both the width and length of the SRR are changed. Also of note is the non-linear dependence of the LC peak evident in Figure 5 a) and b) while in c) the LC has a linear dependence on l_y.

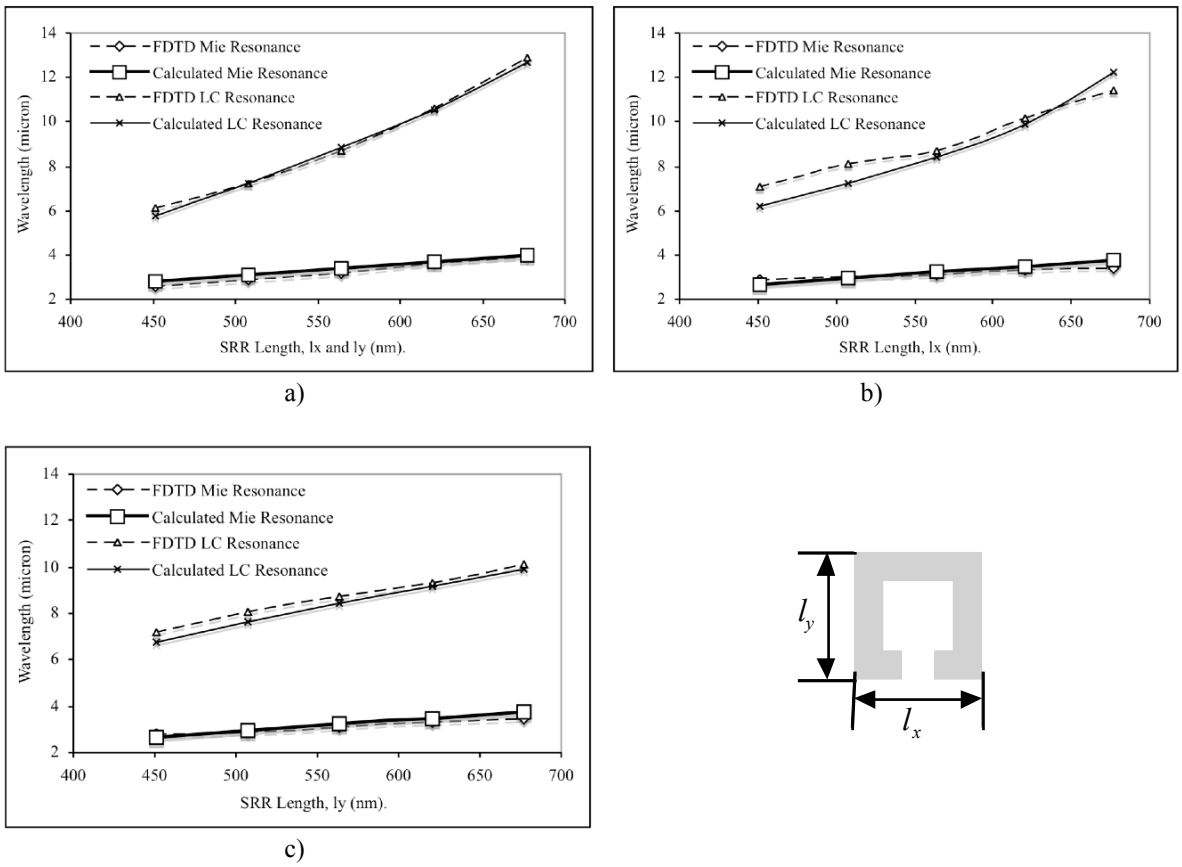

Figure 5. Variation in the Mie and LC resonant frequency as a function of the length of the width, lx, and length, ly, of the SRR element. a) Both lx and ly are changed by equal amount, b) lx is varied and ly is constant and c) ly is varied and lx is constant. All other parameters are constant, a = 750 nm, t= 30 nm, w = 120 nm, g = 130 nm.

5. CONCLUSION.

We have developed a model for the resonant response of an SRR array based on the reduced plasma frequency and the equivalent LC circuit model that provides correlation with experimental and FDTD simulation results for a range of SRR arrays. The techniques provides a relatively straight forward method of predicting the behaviour of a SRR design and enables further understanding to be developed of the dependency of the optical response on the electrical and physical design of the SRR elements. The equations were used to predict the effect of changes in the geometry of an SRR array on the Mie and LC resonant peaks and the results verified by proven FDTD simulations. The model for the LC resonance was refined using the expression for the self and mutual inductances of an SRR element and coplanar capacitance in parallel with the SRR gap capacitance for individual elements and the effective capacitance between neighbouring

elements. The Mie resonance is given by a modified model for the plasma frequency that takes into account the spacing between SRRs and not simply the area dilution factor. The model will be further developed to account for more complex geometries including wire and SRR arrays.

6. ACKNOWLEDGEMENTS

We acknowledge the support of Metamorphose Network of Excellence.

7. REFERENCES

1 Veselago V G 1967 Usp. Fiz Nauk 92 517 or Veselago V G 1968 Sov. Phys – Usp 10 509. (English Translation)

2 M. Notomi, "Negative refraction in photonic crystals." Optical and Quantum Electronics 34: 133–143, 2002.

3 J. B. Pendry "Negative Refraction Makes a Perfect Lens." Phys. Rev. Lett., 85, 3966 (2000).

4 George Goussetis, Alexandros P Feresidis, ShenhongWang,Yunchuan Guo and John C Vardaxoglou, "Uniplanar left-handed artificial metamaterials." J. Opt. A: Pure Appl. Opt. 7 (2005) S44–S50

5 S Linden, C Enkrich, M Wegener,Ji Zhou, Thomas K, C M. Soukoulis "Magnetic response of metamaterials at 100 Terahertz." Science 306, 1351 (2004).

6 Nigel P Johnson, Ali Z Khokhar, Harold M Chong, Chongjun Jin, Jharna Mandel, Scott McMeekin and R M De La Rue, "Increasing Optical Metamaterials Functionality." Proc. SPIE 5955 59550O-1-59550O-6 (2005). Metamaterials Ed Tomasz Szoplik, Ekmel Ozbay, Costas M Soukoulis, Nikolay I Zheludev

7 C. Enkrich, M. Wegener,1 S. Linden, S. Burger, L. Zschiedrich, F. Schmidt, J. F. Zhou, Th. Koschny, and C. M. Soukoulis, "Magnetic Metamaterials at Telecommunication and Visible Frequencies". Phys. Rev. Lett. 95, (2005)

8 C. Rockstuhl, F. Lederer, C. Etrich, T. Zentgraf and J. Kuhl and H. Giessen "On the reinterpretation of resonances in split-ring-resonators at normal incidence". Optics Express, 14, pp8827-8836 (2006)

9 N. Katsarakis, T. Koschny, M. Kafesaki, E. N. Economou and C. M. Soukoulis, "Electric coupling to the magnetic resonance of split ring resonators", Appl. Phys. Lett., 84, pp2943-2945 (2004)

10 Averitt, R.D.; Chen, H.-T.; Taylor, A.J.; Highstrete, C.; Lee, M.; Padilla, W.J. "Dynamical Metamaterials at Terahertz Frequencies" Lasers & Electro-Optics Society, Oct. 2006 pp480-481

11 Zahn M, "Electromagnetic Field Theory" pp343, John Wiley & Sons, 1979.

12 Grover F. W. "Inductance Calculations, Working Formulas and Tables", pp 35 Dover Pub. 1946.

13 Wen C. P. "Coplanar waveguide: A Surface Strip Transmission Line Suitable for Nonreciprocal Gyromagnetic Device Applications." IEEE Trans Microwave Theory Tech. MTT-17, pp1087-1090 (1969).

14 J B Pendry, A J Holden, D J Robbins and W J Stewart, "Low frequency plasmons in thin-wire structures." J. Phys.: Condens. Matter 10, pp4785- 4809 (1998).

15 D. Wu, N. Fang, C. Sun and X Zhang. "Fabrication and Characterisation of THz Plasmonic Filter", Nanotechnology 2002, pp229-231, (2002)

16 RSoft Design Group 400 Executive Blvd. Suite 100 Ossining, NY 10562